A Model γ-Al$_2$O$_3$-Supported Re–Pt Catalyst Prepared from [Re$_2$Pt(CO)$_{12}$]

I. Synthesis and Spectroscopic Characterization

A. S. Fung,* M. R. McDevitt,* P. A. Tooley,* M. J. Kelley,†
D. C. Koningsberger,‡,§ and B. C. Gates*,1

*Center for Catalytic Science and Technology, Department of Chemical Engineering, University of
Delaware, Newark, Delaware 19716; †E. I. du Pont de Nemours and Company, Engineering Technology
Laboratory, Experimental Station, Wilmington, Delaware 19898; ‡Laboratory for Inorganic Chemistry and
Catalysis, Eindhoven University of Technology, P.O. Box 513, 5600 MB Eindhoven, The Netherlands; and
§Debye Institute, Laboratory of Inorganic Chemistry and Catalysis, University of Utrecht, P.O. Box 80083,
3508 TB Utrecht, The Netherlands

Catalysts supported on γ-Al$_2$O$_3$ were prepared from [Re$_2$Pt(CO)$_{12}$], and from Pt (NH$_3$)$_4$(NO$_3$)$_2$ and NH$_4$ReO$_4$. The former samples were characterized by infrared and X-ray photoelectron spectroscopies (XPS) and by temperature-programmed reduction (TPR); the latter were characterized by TPR. [Re$_2$Pt(CO)$_{12}$] was initially chemisorbed on the γ-Al$_2$O$_3$ surface. Upon treatment in H$_2$ at about 150°C, the cluster fragmented and formed rhenium subcarbonyls, and at about 400°C the sample was decarbonylated. Adsorption of CO and of NO as probe molecules gave evidence of metallic Pt, but there was no evidence of adsorption on Re. The XPS data indicating the Re binding energies give evidence of the presence of low-valent cationic Re in the sample after the treatment at 400°C in H$_2$. In contrast, when a mixture of samples of Re on γ-Al$_2$O$_3$ and Pt on γ-Al$_2$O$_3$ prepared from [H$_3$Re$_3$(CO)$_{12}$] and [(CH$_3$)$_2$Pt(COD)], respectively, was treated under equivalent conditions, the Re was present in a high-valent cationic form (Re^{7+}), and Pt was metallic. It is concluded that Pt facilitated the reduction of Re and that Pt was likely near the rhenium in the sample prepared from [Re$_2$Pt(CO)$_{12}$]. The TPR data are consistent with the foregoing results. The TPR data characterizing the samples prepared from the metal salts show that the degree of hydroxylation the γ-Al$_2$O$_3$ support significantly influenced the reduction of the Re and the Pt, but these data are not sufficient to determine the interactions between the two metals. © 1993 Academic Press, Inc.

INTRODUCTION

The reforming of naphtha to give high-octane-number gasoline is catalyzed on a large scale by Pt supported on alumina (Pt/γ-Al$_2$O$_3$) (1). The most widely used reforming catalysts also contain Re (2), which improves activity maintenance and allows economical low-pressure operation that favors aromatic products. Like most solid catalysts used industrially, Re-Pt/γ-Al$_2$O$_3$ is structurally nonuniform and difficult to

characterize, and the structure is sensitive to the method of preparation and pretreatment. The Re- and Pt-containing structures and the role of Re in maintaining the activity are poorly understood. The goal of this research was to use [Re$_2$Pt(CO)$_{12}$] to prepare structurally simple Re-Pt/γ-Al$_2$O$_3$ catalysts, to characterize them structurally, and to understand the role of Re.

[Re$_2$Pt(CO)$_{12}$] was chosen to be a catalyst precursor because it could be activated under mild conditions by removal of the CO ligands. The bonding of the Pt and Re in the precursor cluster was expected to favor the interaction of the two metals during the activation and thus favor the existence of bime-

1 To whom correspondence should be addressed at: Department of Chemical Engineering, University of California, Davis, CA 95616.

190

tallic interactions in the final form of the catalyst. The absence of ligands such as chloride was expected to minimize the complexity of the surface structures and simplify the characterization. For comparison, catalyst samples were also made conventionally with salt precursors.

In this paper, the synthesis and characterization of the catalyst by the following methods are reported: infrared (IR) and X-ray photoelectron spectroscopy (XPS), and temperature-programmed reduction (TPR). In a subsequent paper (3) the performance of the catalyst in a model reforming reaction, the dehydrogenation of methylcyclohexane, is to be reported and compared with that of the conventionally prepared catalyst, and in the third paper (4), characterization of the catalyst by X-ray absorption spectroscopy is to be reported with a model of the structure, and the complete set of results is to be used to postulate a role of the Re.

EXPERIMENTAL METHODS

Reagents and Synthesis of Precursors

Sample preparation and handling were performed under inert atmospheres in a Vacuum Atmospheres drybox, on a double manifold Schlenk vacuum line, and in N_2-filled transfer vessels. $[H_3Re_3(CO)_{12}]$, $[Re(CO)_3OH]_4$, and $[(CH_3)_2Pt(COD)]$ (COD is cyclooctadienyl) were synthesized by the literature methods (5–7). $[Re_2Pt(CO)_{12}]$ was synthesized by a modification of the literature method (8), as follows: $[HRe(CO)_5]$ was synthesized from $[Re(CO)_5Br]$ (9) (1.84 g, 4.53 mmol) and vacuum distilled via a 1-in bed of P_2O_5 into a 100-ml Schlenk flask immersed in liquid N_2. The distillation was almost complete in about 10 h, and the system was charged with CO (Matheson, research grade). $[(CH_3)_2Pt(COD)]$ (0.22 g, 0.65 mmol) was dissolved in freshly distilled hexanes, degassed, and transferred by cannula into the Schlenk flask containing the frozen $[HRe(CO)_5]$, which was then slowly warmed to room temperature, with the contents of the flask changing from creamy yel-

low to dark purple with the formation of a red precipitate. The solution was stirred under static CO for 24 h, and the red precipitate of $[Re_2Pt(CO)_{12}]$ was purified and recrystallized according to the literature method (8). This synthesis has the benefit of a better exclusion of moisture than the literature method and prevents exposure to the toxic, volatile $[HRe(CO)_5]$. The yield of $[Re_2Pt(CO)_{12}]$ was 74% based on Pt vs 84% reported in the literature (8).

Tetrahydrofuran (THF), cyclohexane, and hexanes (reagent grade) were dried and distilled from sodium benzophenone ketyl. Anhydrous diethyl ether was dried over Na/K alloy. $[Re_2(CO)_{10}]$ and K_2PtCl_4 were obtained from Strem and used as received. 1,5-Cyclooctadiene (Gold Label) and methyllithium (1.4 M in diethyl ether) (Aldrich) were used without purification. H_2 (99.999%), He (99.999%), and CO (UHP) were supplied by Matheson. H_2 and He flowed through Cu_2O and activated 4A zeolite traps to remove traces of O_2 and moisture, respectively. CO passed through a γ-Al_2O_3 trap at 300°C and a 4A zeolite trap to remove metal carbonyls and moisture, respectively. O_2 (extra dry grade, Matheson) was used without further purification.

Catalyst Preparation

The γ-Al_2O_3 support (Degussa, Aluminum Oxide C) was made into a paste by adding deionized distilled water, followed by drying at 120°C overnight. It was ground, sieved to give 200–400 μm particles, calcined at 500°C for 2 h, and evacuated (pressure < 10^{-3} Torr) at 500°C overnight. The alumina surface was partially dehydroxylated, and the resulting support material had a surface area of 104 m^2/g (determined by the BET method) and was stored in the drybox before use.

In a standard preparation, the organometallic precursor was brought in contact with partially dehydroxylated γ-Al_2O_3 by slurrying in a freshly distilled solvent {THF for $[Re_2(CO)_{10}]$, hexanes for $[H_3Re_3(CO)_{12}]$ and $[(CH_3)_2Pt(COD)]$} for 4 h. The solvent was

then pumped off and the solid dried in vacuo overnight. The sample was then stored under dry N_2.

Samples with total metal loadings of 1 wt% were typically used in the IR experiments; a Re loading of 1 wt% and a Pt loading of 0.56 wt% were typical of the samples used in XPS and TPR experiments.

Several catalysts (0.8 wt% Re/γ-Al$_2$O$_3$; 0.36 wt% Pt/γ-Al$_2$O$_3$, 0.32 wt% Pt, 0.60 wt% Re/γ-Al$_2$O$_3$; 0.56 wt% Pt, 1.0 wt% Re/γ-Al$_2$O$_3$) were prepared by the incipient wetness technique with aqueous solutions of Pt(NH$_3$)$_4$(NO$_3$)$_2$ (Strem) and NH$_4$ReO$_4$ (Alfa). The resulting solids were allowed to stand overnight at ambient temperature followed by drying at 120°C for 12 h. After calcination in air at 500°C for 2 h, Pt/γ-Al$_2$O$_3$ and Re-Pt/γ-Al$_2$O$_3$ were stored in closed containers before use. The calcined Re/γ-Al$_2$O$_3$ was subsequently treated in flowing N_2 (99.99%) at 500°C for 2 h to increase the dispersion (10).

The metal contents of the samples were determined by X-ray fluorescence spectroscopy with a Philips PW 1410/80 automated X-ray spectrometer.

Characterization of Surface Metal-Containing Species

Strategy of the spectroscopic experiments. Spectroscopic methods were used to examine the structures of the cluster-derived supported metal catalysts at different stages of preparation. The strong absorptions of the carbonyl ligands of the organometallic clusters in the IR spectra provide comparisons of the complexes in solution with those on the γ-Al$_2$O$_3$ surface. The structural evolution of the supported metal carbonyl clusters in H_2 was followed by *in-situ* IR spectroscopy. After reduction of the sample in H_2, CO was used as a probe and chemisorbed on the samples at 50°C to help determine the structure of the supported metal.

XPS was used to provide information about the Re $4f$ binding energies, which are related to the oxidation state of Re surface

species. The partial overlap of the Al $2p$ and Pt $4f$ XP peaks hinders the determination of the Pt oxidation state, and no useful results were obtained for Pt with this method. The reduction behavior of the samples was further characterized in TPR experiments.

Infrared spectroscopy. IR spectra were measured with a Nicolet 7199 Fourier transform spectrometer with a spectral resolution of 2 cm^{-1}. Solution spectra were obtained with a 0.2-mm CaF$_2$ cell. Solid samples were pressed at a pressure of 10,000 psi into self-supporting wafers and characterized in a controlled-environment quartz cell with NaCl windows. The IR cell was connected to a gas manifold so that the sample could be treated in gaseous environments or under vacuum.

The structural evolution of the surface species derived from the organometallic precursors on partially dehydroxylated γ-Al$_2$O$_3$ under H_2 was characterized by the IR absorption in the ν_{CO} region. Each sample was heated from ambient temperature to 400°C in 50°C intervals and then reduced further in H_2 at 400°C for 4 h. After the sample had been cooled in flowing H_2, CO (used as a probe molecule) was allowed to chemisorb on the sample at 50°C followed by evacuation before a spectrum was measured. The resulting carbonyl bands were used to characterize the structures after reduction. The reducibility of Re and Pt in the alumina-supported samples prepared from [Re$_2$Pt(CO)$_{12}$] (1 wt% Re + Pt), [H$_3$Re$_3$(CO)$_{12}$] (1 wt% Re), and [(CH$_3$)$_2$Pt(COD)] (0.88 wt% Pt) was investigated.

X-ray photoelectron spectroscopy. The experiments were carried out with a Physical Electronics AES/XPS spectrometer (Model 551) equipped with an Al K_α anode (10 kV, 60 mA, 1486.6 eV) and a cylindrical mirror analyzer. The base pressure of the instrument was always $< 5 \times 10^{-9}$ Torr, with typical operating pressures being $< 5 \times 10^{-8}$ Torr. Samples were ground and mounted as powders by packing into an aluminum holder with a 1-cm diameter $\times$ 1-mm

deep cavity with an aluminum hand press. The sample was attached to a heatable sample transfer probe. Each sample was transferred from the drybox to the prechamber of the spectrometer under a nitrogen blanket in an 8-liter plastic bag. The prechamber was connected to a turbomolecular pump and a gas manifold so that the samples could be subjected to *in-situ* gas treatments and evacuation.

In a typical experiment, the sample was first evacuated at room temperature in the prechamber to remove traces of physisorbed moisture. It was then reduced in flowing H_2 at 400°C for 2 h (flow rate = 100 ml (NTP)/min, heating rate = 5°C/min). After the sample had cooled, the prechamber was evacuated to a pressure $< 10^{-6}$ Torr and the sample introduced into the ultrahigh vacuum chamber. Data were collected overnight to maximize the signal to noise ratio. The C_{1s} peak at 284.6 eV was used to determine the binding energy of the reference compounds. The Al_{2p} peak at 74.5 eV was used as the internal reference, and the C_{1s} binding energy was used to check the internal consistency of the binding energy assignments. Re foil (Ar⁺ sputtered), [Re(CO)₃OH]₄, ReO_2, and Re_2O_7 were used to characterize the binding energies of Re(0), Re(I), Re(IV), and Re(VII), respectively. To avoid the decomposition of [Re(CO)₃OH]₄, it was mounted on indium foil and cooled to liquid nitrogen temperature during data acquisition.

Alumina-supported samples prepared from [H₃Re₃(CO)₁₂] and [Re₂Pt(CO)₁₂] were reduced *in situ*, and the XP spectra measured. A mechanical mixture of equal masses of an alumina-supported sample prepared from [H₃Re₃(CO)₁₂] (1.4 wt% Re) and an alumina-supported sample prepared from [(CH₃)₂Pt(COD)] (0.88 wt% Pt) was used to investigate the effect of the proximity of Pt on the reducibility of Re.

Temperature-programmed reduction. The TPR experiments were carried out with 4% H_2 in Ar or 5% O_2 in He, flowing over samples of about 0.3 to 0.4 g of catalyst in

appartus described by Huizinga *et al.* (*11*). H_2, Ar, and He were purified by flowing through a zeolite 4A trap and a trap containing Cu_2O to remove residual water and O_2, respectively. O_2 passed through a zeolite 4A trap to remove moisture. A thermal conductivity detector (TCD) was used to determine the difference in the O_2 and H_2 concentrations of the gas mixture upstream and downstream of the reactor. The TCD signal was measured and integrated as a function of temperature so that the temperature-programmed reduction and oxidation spectra were recorded. Before entering the thermal conductivity cell, the reactor effluent flowed through a trap containing zeolite 4A to remove water formed during reduction. The uncertainty in H_2 consumption was estimated to be 10%. All samples, unless otherwise specified, were first dried at 120°C in He for 1 h before the reduction treatment.

The samples consisting of 1.0 wt% Re on γ-Al₂O₃, 0.8 wt% Pt on γ-Al₂O₃, and 1.0 wt% Re + 0.56 wt% Pt on γ-Al₂O₃ prepared from salt precursors were first subjected to the following reduction treatments with a total flow rate of 5 ml/min in all cases: (1) The sample was flushed with Ar at 25°C; (2) Ar was then replaced by a 4% H_2 in Ar mixture, causing the appearance of the switching peak; (3) after the TCD signal stabilized, the sample was heated at 10°C/min to 500°C and held at 500°C for 4 h; (4) the sample was cooled in 4% H_2 to 25°C.

After the sample had been cooled in 4% H_2 in Ar, it was oxidized in a controlled fashion (passivated) at room temperature by first passing He for 12 h followed by pulses of O_2 (each 3 μl) at one-minute intervals into a He stream (5 ml/min) for 2 h. Then the sample was oxidized with a flowing stream of 4% O_2 in He for another hour. The passivated sample was stored at room temperature for 24 h followed by drying in He at 120°C for 1 h. A TPR experiment was then conducted to determine the reducibility of the supported metals. The heating profile for the TPR experiment is illustrated in Fig. 1.
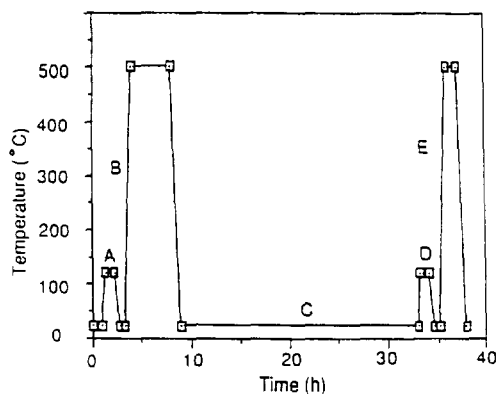
FIG. 1. The heating profile for the TPR experiment: (A, D) drying; (B) first TPR, (C) passivation, and (E) second TPR.

Samples prepared by adsorbing [H$_3$Re$_3$(CO)$_{12}$] (1.2 wt% Re) and [Re$_2$Pt (CO)$_{12}$] (1.0 wt% Re, 0.56 wt% Pt) on γ-Al$_2$O$_3$ were subjected to TPR over the range 25 to 500°C with a heating rate of 5°C/min. The samples were then passivated, dried, and reduced as stated above for the catalysts prepared from salt solutions.

RESULTS AND DISCUSSION

Characterization of the Sample Formed by Adsorption of [Re$_2$Pt(CO)$_{12}$] on γ-Al$_2$O$_3$

The dark purple THF solution of [Re$_2$Pt(CO)$_{12}$] became colorless after stir-

ring at room temperature for 4 h with γ-Al$_2$O$_3$. The solid attained a dark brown color, and, after drying under vacuum overnight, it had a rust color. Since the sample was sensitive to air (turning gray in air), all sample handling and preparations were performed under dry nitrogen. The IR spectrum of the resultant supported cluster (Fig. 2A) is similar to that of [Re$_2$Pt(CO)$_{12}$] in THF (Table 1). There was a slight shift to lower energy in the IR spectrum as a result of adsorption, and the peaks became broadened, which is typical of supported organometallics. New, weak bands appeared at 2128, 2091, and 1907 cm^{-1}. The new features observed in the spectrum of the solid are similar to those reported for samples prepared adsorption of [Re$_2$Pt(CO)$_{12}$] on γ-Al$_2$O$_3$ (15).

The similarity of the carbonyl IR spectra of [Re$_2$Pt(CO)$_{12}$] and [Re$_2$(CO)$_{10}$] in THF and their respective solid-state spectra can be explained by a vibrational analysis of the C–O stretching frequencies in each carbonyl cluster on the basis of symmetry arguments. Flitcroft et al. (16) performed a vibrational analysis and showed that [Re$_2$(CO)$_{10}$] has three IR-active C–O stretching modes, $2B_2$ and E_1, with the energies being $B_2 > E_1 > B_2'$. Although the point groups of [Re$_2$(CO)$_{10}$] and [Re$_2$Pt(CO)$_{12}$] belong to D_{4d} and D_{2h}, respectively, the local symmetry coordinates for the carbonyl stretching modes of the two [Re(CO)$_5$] moie-

TABLE 1

Infrared Carbonyl Stretching Frequencies of Re and Re–Pt Carbonyl Complexes

Sample	ν_{CO} (cm^{-1})	Reference
[Re$_2$Pt(CO)$_{12}$] in THF	2084 (ms), 2021 (s), 2004 (s, sh), 1975 (m)	This work
[Re$_2$(CO)$_{10}$] in THF	2070 (m), 2012 (s), 1967 (m)	This work
[Re$_2$Pt(CO)$_{12}$] adsorbed on γ-Al$_2$O$_3$	2128 (vw), 2091 (w), 2073 (m), 2026 (sh), 2015 (s), 1997 (sh), 1907 (m br)	This work
[Re$_2$(CO)$_{10}$] adsorbed on γ-Al$_2$O$_3$ ^{a}	2128 (w), 2095 (w), 2074 (s), 2027 (sh), 2015 (s), 1994 (sh), 1916 (vw, br)	This work
[Re$_2$(CO)$_{10}$] adsorbed on γ-Al$_2$O$_3$	2127, 2073, 2015, 2009, 1967	(12)
[Re$_2$(CO)$_{10}$] adsorbed on Y zeolite	2132, 2080, 2025, 2014	(13)

^{a} The three Raman-active CO stretching modes have absorptions at 2128, 2029, and 1993 cm^{-1} (14).
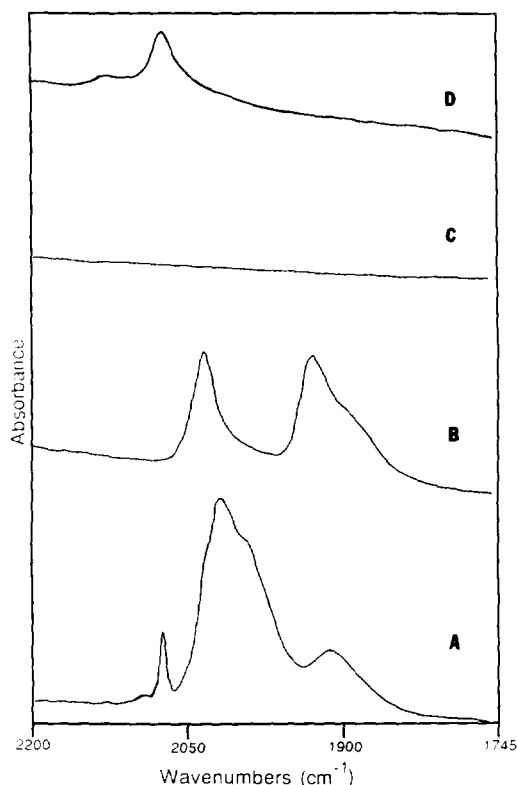
FIG. 2. IR spectra in the ν_{CO} region of (A) sample prepared by adsorption of [Re₂Pt(CO)₁₂] from THF solution onto γ-Al₂O₃ under N₂, (B) after 0.5 h of exposure to H₂ at 1 atm and 150°C, (C) after 2 h of exposure to H₂ at 1 atm and 400°C, and (D) after subsequent CO adsorption at 1 atm and 50°C, followed by evacuation.

ties in each complex can be described by a C_{4v} point group. With this simplification, the [Re(CO)₅] moiety in each complex should have three IR-active C–O stretching modes, $2A_1$ and E. This is consistent with the ν_{CO} pattern observed for metal complexes [M(CO)₅] with square pyramidal structures and [M(CO)₅L] (where L = ligand).

A similar approximate vibrational analysis has been applied to the [Pt(CO)₂] moiety in [Re₂Pt(CO)₁₂]. There is only one IR-active CO stretching mode, B_{2u}, in the D_{2h} local symmetry coordinates for the carbonyl stretching modes of the [Pt(CO)₂] moiety. Therefore, on the basis of the relative inten-

sities and positions of the IR absorptions observed in other [Re(CO)₅L] complexes (Table 1), the bands at 2084, 2021, and 1975 cm⁻¹ are assigned to the three C–O stretching modes of the [Re(CO)₅] moiety. The remaining band at 2004 cm⁻¹ is assigned to the C–O stretching mode of the [Pt(CO)₂] moiety.

The similarities of the relative intensities and positions of the IR absorptions of the [Re(CO)₅] moiety characteristic of [Re₂Pt(CO)₁₂] and [Re₂(CO)₁₀] in THF extend to the respective spectra of the adsorbed species on alumina. The spectrum of the sample formed from [Re₂Pt(CO)₁₂] adsorbed on γ-Al₂O₃ is similar to that of the sample formed from [Re₂(CO)₁₀] adsorbed on γ-Al₂O₃, except for the additional band at 1907 cm⁻¹ (Table 1). New but weak absorptions at 2128, 2095, and 2027 cm⁻¹ appeared in both spectra. These bands in the sample made from [Re₂(CO)₁₀] are Raman active, and their presence is explained by the slight disruption of the symmetry due to the lateral interaction of the dirhenium complex with the support surface. The surface dirhenium complex derived from [Re₂(CO)₁₀] adsorbed on γ-Al₂O₃ could be washed off the support with THF, in agreement with the weak interaction of this compound with the support surface. Therefore, the close agreement of the IR spectrum of the [Re(CO)₅] moiety in [Re₂(CO)₁₀] and that in [Re₂Pt(CO)₁₂] implies that the [Re(CO)₅] moiety interacts weakly with the alumina surface in the Re–Pt carbonyl complex.

Attempts to extract the mixed-metal carbonyl cluster from the surface with THF were not successful. The failure to remove the Re–Pt organometallic from the alumina surface suggests that it had been chemisorbed onto the support surface.

The additional band at 1907 cm⁻¹ is now tentatively assigned to the CO stretching frequency of the [Pt(CO)₂] moiety. The observed downshift from 2004 to 1907 cm⁻¹ suggests that a strong interaction between the [Pt(CO)₂] moiety and the support surface leads to an increase in the π-back dona-

tion from Pt to the π^* antibonding orbital of the CO ligand. Since the [Re(CO)$_5$] moiety in the Re–Pt carbonyl cluster interacted weakly with the alumina surface, the carbonyl cluster probably interacted strongly with the surface via the [Pt(CO)$_2$] moiety, but the exact nature of the interaction is not known.

In summary, the surface species derived from the adsorption of [Re$_2$Pt(CO)$_{12}$] on partially dehydroxylated γ-Al$_2$O$_3$ was chemisorbed. Simple contacting with THF, in which the cluster is soluble, did not remove the organometallic from the alumina surface. This evidence implies that the Re–Pt organometallic cluster interacts strongly with the surface, probably through the [Pt(CO)$_2$] moiety.

Reactivity of the Surface Species Derived from γ-Al$_2$O$_3$-Supported [Re$_2$Pt(CO)$_{12}$] in H$_2$

Characterization by IR spectroscopy. After exposure of the supported mixed-metal cluster to flowing H$_2$ at 150°C for 0.5 h, the initial IR absorptions disappeared, and bands appeared at 2032 (s), 1925 (s), and 1903 (sh) cm^{-1} (Fig. 2B). The band pattern is shifted to higher energy by 10 cm^{-1} but otherwise is in close agreement with the pattern characteristic of a mononuclear Re subcarbonyl species having C_v symmetry, as observed by Kirlin *et al.* (*17*). Kirlin's sample was prepared from alumina-supported [H$_3$Re$_3$(CO)$_{12}$] treated at 225°C in H$_2$ for 4 h. This Re subcarbonyl was formulated as [Re(CO)$_3${O–Al} {HO–Al}$_2$] (*17*). Similar Re subcarbonyls on MgO have been formed from [HRe(CO)$_5$] and characterized by vibrational (*18*) and X-ray absorption (*19*) spectroscopies.

To test our assignment and the formation of the mononuclear Re subcarbonyl surface species from the supported mixed-metal cluster, a sample prepared from [H$_3$Re$_3$(CO)$_{12}$] adsorbed on γ-Al$_2$O$_3$ was reduced in H$_2$ at 150°C for 0.5 h. Nearly the same IR absorption band pattern as that of the sample derived from the supported

mixed-metal cluster was observed [2037 (s), 1925 (s), and 1895 (sh) cm^{-1}], consistent with the suggestion that the mixed-metal cluster had been fragmented upon heating, resulting in the formation of the partially oxidized Re in the form of a subcarbonyl.

The observed surface reaction between the organometallic clusters and the support surface can be understood on the basis of the reactivity of the carbonyl clusters with nucleophiles such as surface hydroxyl and μ-oxo groups (*20*). The spectrum of the Re subcarbonyl surface species persisted with decreasing intensity at higher temperatures.

After reduction at 400°C for 2 h, no carbonyl absorptions were observed for the sample prepared from [Re$_2$Pt(CO)$_{12}$] on alumina (Fig. 2C). Subsequent CO chemisorption at 50°C resulted in carbonyl bands at 2122 (w, br) and 2068 (s) cm^{-1} (Fig. 2D). The 2068 cm^{-1} absorption is assigned to linear CO adsorbed on metallic Pt (*14*). The weak absorption at 2122 cm^{-1} is assigned to CO adsorbed on unknown surface cationic species. As the metal species become more electropositive, there is a decreased tendency for electrons to be transferred to the π^* antibonding orbital of CO from the d-π bonding orbital of the metal, leading to a shift to higher energy in the CO stretching frequency relative to that of linear CO adsorbed on metallic Pt. No carbonyl bands corresponding to bridging carbonyls on Pt or CO adsorbed on metallic Re (2044 cm^{-1}) were observed. The lack of bridging carbonyl absorptions of CO on metallic Pt suggests that the Pt particle or cluster size was small (*21*).

To determine the structure of the Re species in the reduced cluster-derived Re–Pt catalyst, NO was also used as a probe molecule to detect the presence of cationic Re species after CO chemisorption. However, no adsorption was observed in the 1900–1700 cm^{-1} region where stretching frequencies corresponding to NO adsorbed on surface Re species were expected (*22*).

In contrast, after treatment of [H$_3$Re$_3$(CO)$_{12}$] on γ-Al$_2$O$_3$ in H$_2$ at 400°C for

4 h, only a very weak broad absorption in the ν_{CO} region with a peak at 2044 cm^{-1} was observed. This band is assigned to linear CO adsorbed on metallic Re (21, 22) and suggests that only a small fraction of the Re had been reduced to metal under these conditions. This result is consistent with the strong interaction between Re and γ-Al₂O₃ in samples with low Re contents, leading to the low reducibility of γ-Al₂O₃-supported Re catalysts (10).

Another experiment was carried out to investigate the IR band position of CO chemisorbed on metallic Pt. A sample prepared by adsorbing [(CH₃)₂Pt(COD)] on alumina (0.88 wt% Pt) was treated in H₂ at 400°C for 4 h followed by CO adsorption at 50°C. A carbonyl band was observed at 2068 cm^{-1}.

XPS. XPS was used to examine the oxidation state of Re after reduction in both Re and Re–Pt samples derived from organometallic precursors. The binding energies of the Re foil, [Re(CO)₃OH]₄, ReO₂, and Re₂O₇ were measured to characterize the oxidation states of Re(0), Re(I), Re(IV), and Re(VII), which are 40.0, 40.2, 42.5, and 46.4 eV, respectively. Details are given elsewhere (23).

Binding energies corresponding to Re (VII) were detected in the sample of ReO₂, which were probably caused by air oxidation leading to the formation of a surface oxide layer of Re₂O₇. The Re $4f_{7/2}$ binding energy characterizing Re(IV) in ReO₂ was found to be 42.5 eV, which is in close agreement with values reported (Table 2).

The binding energies characteristic of metallic Re and Re(VII) range from 40.0 to 46.4 eV. This wide range allows a clear distinction between Re(0) and Re(VII), but the distinction between Re(0) and Re(I) is not clear. The intense Al₂ₚ line strongly interfered with the Pt $4f_{7/2}$ binding energy [Pt(0) = 70.9 eV]. Therefore, only the 4f binding energies of Re were examined.

Reduction of the sample formed from [Re₂Pt(CO)₁₂] adsorbed on γ-Al₂O₃. Partially oxidized Re surface species were observed after the sample prepared from [Re₂Pt(CO)₁₂] adsorbed on γ-Al₂O₃ had

TABLE 2

XP Binding Energies of Alumina-Supported Re and Re–Pt Samples (24)

Sample	B. E. (eV)	
	Re $4f_{7/2}$	C 1s[a]
Sample prepared by adsorption of [H₃Re₃(CO)₁₂] on γ-Al₂O₃[b]	46.7	284.6
Sample prepared by adsorption of [Re₂Pt(CO)₁₂] on γ-Al₂O₃ treated in H₂ at 250°C	41.3	284.0
Sample prepared by adsorption of [Re₂Pt(CO)₁₂] on γ-Al₂O₃[b]	40.5	284.3
A physical mixture of equal masses of sample prepared by adsorption of [H₃Re₃(CO)₁₂] on γ-Al₂O₃ and sample prepared by adsorption of [(CH₃)₂Pt(COD)] on γ-Al₂O₃[b]	47.7	284.4

[a] Al $2p$ = 74.5 eV is used as the reference binding energy, and the reported C 1s binding energy is reported only as a consistency check.

[b] Sample was heated in H₂ at 400°C for 2 h.

been treated in H₂ at 250°C for 2 h (Fig. 3C). The observed Re $4f_{7/2}$ binding energy of 41.3 eV characterizes Re oxidation states between +1 and +4. Tysoe et al. (25) observed Re species with an approximately 1 eV shift in the binding energy relative to that characteristic of metallic Re (39.7 eV) in their investigation of the oxidation and reduction of Re–Pt thin films. They assigned the binding energy to Re(II). Nguyen et al. (26) also reported a Re $4f_{7/2}$ binding energy of 41.6 eV for ReO. Therefore, the binding energy measured in the present work for Re surface species derived from [Re₂Pt(CO)₁₂] after treatment in H₂ at 250°C is inferred to be consistent with a +2 oxidation state for Re.

After treatment in H₂ at 400°C for 2 h, the Re in the sample was reduced to a lower oxidation state than that which resulted after treatment at 250°C (with a Re $4f_{7/2}$ binding energy of 40.5 eV, Fig. 3D). As the binding energies characterizing Re(0) and Re(I) were 40.0 and 40.2 eV, respectively, and the limit of the experimental accuracy in the measured blinding energy was approxi-
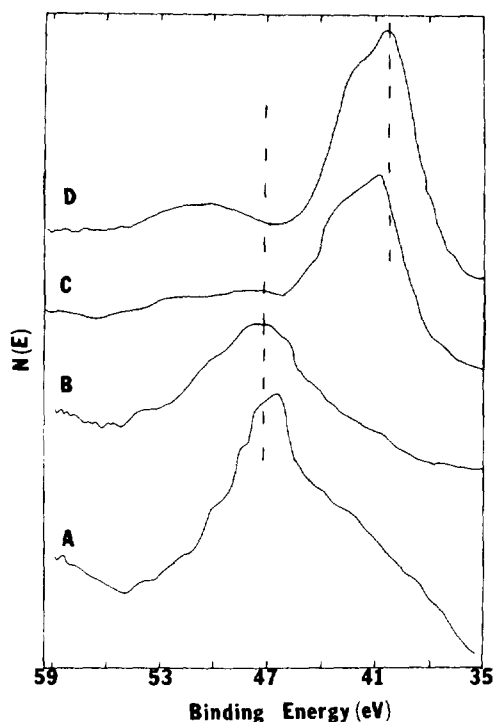
FIG. 3. XP spectra of (A) sample prepared by adsorption of [H₃Re₃(CO)₁₂] on γ-Al₂O₃ after treatment in H₂ at 400°C for 2 h, (B) sample prepared as a physical mixture of equal masses of a sample prepared from [H₃Re₃(CO)₁₂] adsorbed on γ-Al₂O₃ and a sample prepared from [(CH₃)₂Pt(COD)] adsorbed on γ-Al₂O₃ after treatment in H₂ at 400°C for 2 h, (C) sample prepared by adsorption of [Re₂Pt(CO)₁₂] on γ-Al₂O₃ after treatment in H₂ at 250°C for 2 h, and (D) sample prepared by adsorption of [Re₂Pt(CO)₁₂] on γ-Al₂O₃ after treatment in H₂ at 400°C for 2 h.

explained in terms of the final state effect (*31, 32*). The upshift in the binding energy relative to that characteristic of bulk Re metal (B.E. = 40.0 eV) is caused by the ineffectiveness of small supported metal crystallites in screening the core-hole after the photoelectrons are ejected. This slightly positively charged core-hole gives an upshift in the observed binding energy.

(2) Re exists as low-valent cationic species. The reference compound [Re(OH)(CO)₃]₄, with Re in a formal oxidation state of +1, was found to have a binding energy of 40.2 eV. The observed binding energy of 40.5 eV for the surface species derived from reducing the sample formed from [Re₂Pt(CO)₁₂] is equal to this value within the experimental error. The strong

TABLE 3

XP Binding Energies of Re and Re–Pt Samples

Sample	B. E. (eV)		Ref.
	Re $4f_{7/2}$	C 1s	
Re–Pt alloy (60% Re, 40% Pt)[a]	40.6	—	(28)
Ten monolayers of Re on Pt (111)[b]	40.4	—	(29)
Ten monolayers of Re on Pt (111) followed by annealing to 877°C[b]	40.8	—	(29)
Sample of Re–Pt catalyst (2.7% Re, 2.4% Pt) prepared from salt precursors[c]	42.5	284.6[d]	(27)
Sample of Re–Pt catalyst (0.9% Re, 0.9% Pt) prepared from salt precursors[c]	42.2	285.6[f]	(30)

[a] Au $4f_{7/2}$ = 84 eV is used as the reference binding energy.
[b] Pt $4f_{7/2}$ = 70.9 eV is used as the reference binding energy.
[c] Sample heated in H₂ at 500°C for 4 h.
[d] C1s = 284.6 eV is used as the reference binding energy.
[e] Sample heated in H₂ at 485°C.
[f] Al 2p = 74.5 eV is used as the reference binding energy, and the reported C 1s binding energy is stated only as a consistency check.

mately 0.3 eV, the assignment of the formal oxidation state of the Re surface species is difficult. For comparison, Re binding energies for conventionally prepared Re–Pt catalysts treated in H₂ (*27*) and those reported for a Re–Pt alloy are also included in Table 3.

There are several candidates for the Re surface species having a binding energy of about 40.5 eV in the sample prepared from the mixed-metal cluster:

(1) Re may be in the metallic state. Shifts of ca. 0.5 eV have been observed for other highly dispersed metal catalysts and were

interaction between Re and the oxide support might prevent the complete reduction of Re in the presence of H_2 at 400°C. In most XPS investigations of alumina-supported Re–Pt catalysts, the Re binding energy has been found to be greater than 40.5 eV after reduction at 500°C *(27, 30, 33)*. Furthermore, Re is an oxophilic metal and may become cationic as a result of polar interactions. These polar interactions may be analogous to the interactions of Re with oxygen induced by O_2 adsorption on Re–Pt alloy, which leads to partial oxidation of Re *(31, 40)*.

(3) Re and Pt form a bimetallic surface alloy. XP spectra characterizing a Re–Pt alloy (60% Re, 40% Pt) showed a Re $4f_{7/2}$ binding energy of 40.6 eV *(28, 29)*. The upshift in the binding energy may be attributed to the electronic interaction between the two metals. The XP binding energy of Re in a reduced SiO_2-supported Re–Pt sample was also found to be 40.7 ± 0.1 eV, which is 0.2 eV higher than that measured for reduced SiO_2-supported Re *(35)*. Therefore, it is inferred that the electronic interaction between Re and Pt would result in a higher Re binding energy than that characteristic of metallic Re.

These possibilities can be evaluated on the basis of the IR results. Case (3) can be rejected because the frequency of linearly adsorbed CO on Pt was the same for the sample prepared from $[Re_2Pt(CO)_{12}]$ and that prepared from $[(CH_3)_2Pt(COD)]$ on γ-Al_2O_3 after reduction. If there had been electronic interactions between Re and Pt, there would have been a difference in these frequencies *(35)*. Furthermore, we did not observe any linearly adsorbed carbonyls that would indicate the presence of metallic Re. Although the extinction coefficient of CO adsorbed on metallic Re might be less than that of CO on Pt, the high Re to Pt ratio in the cluster-derived catalyst suggests that linearly adsorbed CO on metallic Re would have been observed if it had been present in substantial concentrations *(21, 22)*. On the

other hand, no cationic species were observed by NO adsorption. Therefore, it is suggested that the Re adsorption sites may have been modified after reduction, and it is not possible to exclude the existence of either metallic Re [Case (1)] or cationic Re [Case (2)] after reduction.

The facilitation of the reduction of Re by Pt in the cluster-derived catalyst suggests that the two metals were in close proximity. The interaction between them might indicate the presence of Re–Pt ensembles or of hydrogen spillover. To assess the possibility that the two metals must be in close proximity for the ease of reduction of Re, a sample in which the Re and Pt were widely separated (consisting of a physical mixture of equal masses of a sample of γ-Al_2O_3-supported $[H_3Re_3(CO)_{12}]$ and a sample of γ-Al_2O_3-supported $[(CH_3)_2Pt(COD)]$) was prepared and reduced under the conditions stated above for the sample prepared from $[Re_2Pt(CO)_{12}]$. The average Re binding energy was found to be 47.7 eV, indicating a mixture of species with Re oxidation states between +4 and +7 (Fig. 3B). The average oxidation state of Re in this mixture was almost the same as that of the Re surface species derived from $[H_3Re_3(CO)_{12}]$ on γ-Al_2O_3 after treatment in H_2, but it was markedly higher than that in the sample prepared from $[Re_2Pt(CO)_{12}]$. Since the γ-Al_2O_3 used in all three samples had been predried at the same temperature, they all had the same degree of hydroxylation and presumably the same resistance to transport of surface species. Thus we infer that the Pt-facilitated reduction of Re does depend on the proximity of Re and Pt.

In summary, it is concluded from the XP spectra that the sample prepared from $[Re_2Pt(CO)_{12}]$/γ-Al_2O_3 after H_2 treatment incorporated Re in a low-valent form. However, it is unclear whether Re existed in the +1 or the zerovalent state. Pt facilitates the reduction of Re, and it is inferred that Pt was likely near Re in the sample derived from $[Re_2Pt(CO)_{12}]$. When combined with

the IR results, the XP spectra lead to the speculation that Pt may lie atop the Re and block adsorption on it.

TPR. To confirm the ease of reduction of Re and the homogeneity of the surface species, TPR experiments were carried out with the samples derived from [Re$_2$Pt(CO)$_{12}$] and from [H$_3$Re$_3$(CO)$_{12}$] adsorbed on alumina after controlled oxidation. TPR has been applied frequently to characterize interactions between metals in supported bimetallic catalysts (*36*). The method is sensitive to differences in the reducibility among samples, helping to differentiate the structures in supported metal catalysts (such as metal crystallites and metal oxides) and to characterize the metal–O bond strengths in samples with very low metal contents. Several investigators have attempted to use TPR to elucidate the structure and the interactions of Re and Pt in supported catalysts (*37–41*). The interaction between the two metals has been found to be influenced by the Re loading (*42–44*), the ratio of the two metals (*37*), the chloride content (*45*), the water partial pressure in the H$_2$ used for reduction (*38, 42–44*), and, especially, the temperature of the drying or calcination preceding reduction (*37–39, 44*). When an alumina-supported Re–Pt sample prepared from salt precursors was dried at temperatures below 200°C, TPR showed that the coreduction of the two metals occurred at a temperature intermediate between those characteristic of the two monometallic counterparts (*37–39*). In contrast, when the catalyst was dried or preoxidized at 500°C, two separate reduction peaks were observed. The reduction profile was similar to the sum of the individual profiles of the alumina-supported Re and the alumina-supported Pt. The results were explained by the interaction of Re and Pt caused by the high mobility of the Re oxide on the hydroxylated alumina surface, leading to the formation of Re–Pt aggregates during reduction (*37, 38*). In contrast, dehydroxylation at high temperature suppressed the mobility of Re oxide, and consequently the Re could be reduced

only at high temperatures; the reduction profile is similar to that of monometallic Re on alumina (*37, 39*).

The catalytic nature of the reduction was demonstrated by Ziemecki *et al.* (*46*) with Re$_2$O$_7$ on palladium black; the reduction of Re$_2$O$_7$ occurred at temperatures well below 200°C, resulting in the formation of Re–Pd alloy. Mieville (*41*) also demonstrated a catalyzed reduction of Re oxide, but in a physical mixture of Pt on alumina and Re on alumina. He therefore proposed that Pt acts as an initial site for hydrogen spillover. The activated hydrogen was inferred to facilitate the reduction of the neighboring Re oxide to give metallic Re, which then could act as a catalyst for the reduction of the remaining oxide. The rate is influenced by the hydrogen transfer on the alumina surface, which is controlled by the degree of hydroxylation. Mieville argued that a Re–Pt "alloy" is not a necessary requirement for the observed coreduction.

The observed catalyzed reduction of Re is a manifestation of hydrogen spillover. A reference frequently quoted to argue against the spillover phenomenon is that of Isaacs and Petersen (*39*). They showed that hydrogen spillover from Pt alone could not produce enough active hydrogen under their conditions to account for the reduction of Re, but they did not account for the autocatalytic effect once Re oxide is converted to metallic Re to become a new reduction catalyst.

In the present work, TPR of samples prepared from the mixed-metal cluster and samples prepared from salt precursors was used in attempts to understand the reducibility of Re and Pt, the homogeneity of the resulting surface species, and the possible interactions between the two metals after reduction. Experiments were carried out with the catalysts derived from [Re$_2$Pt(CO)$_{12}$] (0.56 wt% Pt, 1.0 wt% Re) adsorbed on γ-Al$_2$O$_3$ and [H$_3$Re$_3$(CO)$_{12}$] (1.2 wt% Re) adsorbed on γ-Al$_2$O$_3$, which had been previously reduced at 500°C for 4 h followed by controlled oxidation (passivation) at room

temperature. The reduction profiles were compared with those obtained for the passivated samples prepared from salt precursors, Re on γ-Al$_2$O$_3$ (0.8 wt% Re), Pt on γ-Al$_2$O$_3$ (0.8 wt% Pt), and Re–Pt on γ-Al$_2$O$_3$ (0.56 wt% Pt, 1.0 wt% Re). The salt-derived samples had been prereduced at 500°C and oxidized carefully at room temperature (passivated). Previous TPR investigations of Re–Pt catalysts have shown that by oxidizing a reduced, conventionally prepared Re–Pt sample at approximately 100°C, the intimacy of the two metals can be maintained (37). Precautions were taken to dry each sample at 120°C in He before the second reduction to maintain a comparable surface hydroxyl group content from one sample to another. This approach of investigating the passivated, prereduced cluster-derived samples alleviated the complications caused by the evolution of CO, CO$_2$, and/or CH$_4$ resulting from the reaction of the carbonyl ligands with the support and the gas atmosphere during the initial reduction step. Otherwise, with the TCD it would not be possible to distinguish the H$_2$ consumption from the evolution of other gases, making the actual rate of H$_2$ consumption difficult to determine.

The interpretation of reduction profiles measured in the TPR of passivated noble metals is usually based on the assumptions that, during the room-temperature passivation, oxygen is adsorbed dissociatively, but that full oxidation does not occur (11). The surface of a noble metal particle is usually assumed to be covered, with an O/M surface ratio of 1. In the second reduction after passivation, H$_2$ can diffuse through the oxide layer to the metal core at low temperature. H$_2$ is activated by the inner metal core and causes the reduction of the surface oxide layer. The temperature corresponding to the maximum rate of H$_2$ consumption becomes lower than that characteristic of the sample prior to passivation. The amount of H$_2$ needed to titrate off the adsorbed surface oxygen is correlated with the dispersion of the metal, since a highly dispersed sample

is expected to chemisorb more O$_2$ than a sample with low dispersion during passivation. Information about the particle or cluster size distribution could be inferred from the broadness of the peak.

The H$_2$ consumption in each reduction experiment was calculated by integration to determine the area under the reduction profile. The oxidation states of Re and Pt have been estimated from the calculated amount of H$_2$ needed to reduce Re and Pt in various oxidation states. The stoichiometric amount of H$_2$ needed to convert each species to the zerovalent form was then calculated from the metal loading of each sample. Since the initial metal oxidation states were not known exactly, the results stated in this form should be judged with caution; the data represent only the apparent H$_2$ consumption/emission (47). Other contributions, such as adsorption, spillover, desorption of chemisorbed hydrogen, and desorption of spillover hydrogen have not been considered, and thus the H$_2$ consumption data may not provide a direct measure of the true extent of the reduction of the metals.

The reduction behavior of γ-Al$_2$O$_3$-supported Pt. The reduction profile of the calcined 0.8 wt% Pt on γ-Al$_2$O$_3$ sample shows a maximum at 230°C with a shoulder at 380°C (Fig. 4A). The temperature corresponding to the maximum rate of reduction is consistent with those reported (11, 37, 39). Huizinga et al. (11) observed a similar reduction profile for a 5 wt% Pt on γ-Al$_2$O$_3$ sample after it had been oxidized at 200°C, assigning the low-temperature peak to the easily reduced PtO$_2$ particles and the high-temperature peak to isolated Pt cations. The H$_2$ consumption of the 0.8 wt% Pt sample was determined to be 82 μmol of H$_2$/g of catalyst and corresponds to a complete reduction from Pt(IV) to Pt(0) (Table 4). In the second reduction after passivation, H$_2$ consumption had already been observed and completed at room temperature. The amount of H$_2$ uptake was 45 μmol of H$_2$/g of catalyst and is in agreement with a complete reduction of all
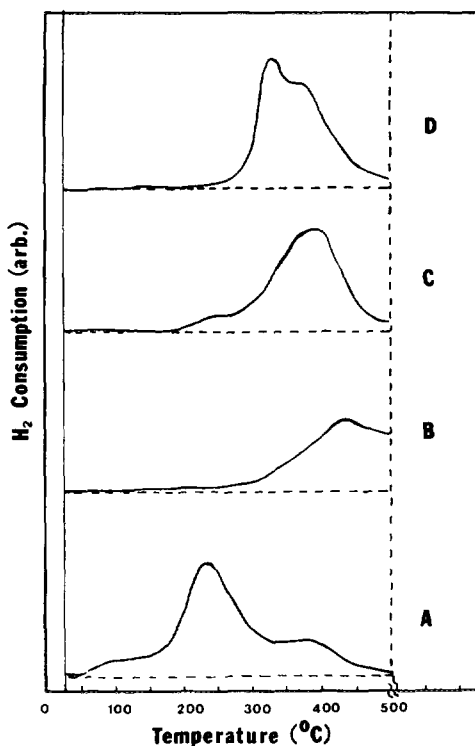
FIG. 4. TPR profiles for (A) calcined Pt on γ-Al$_2$O$_3$ prepared from Pt(NH$_3$)$_4$(NO$_3$)$_2$, (B) calcined Re on γ-Al$_2$O$_3$ prepared from NH$_4$ReO$_4$, (C) passivated sample of Re on γ-Al$_2$O$_3$ prepared from NH$_4$ReO$_4$, and (D) passivated sample of Re on γ-Al$_2$O$_3$ prepared from [H$_3$Re$_3$(CO)$_{12}$] after H$_2$ treatment.

the Pt in the sample from Pt(II) to Pt(0) (Table 4).

Since the consumption of H$_2$ was complete at room temperature, the amount of H$_2$ uptake might instead be interpreted as the sum of that consumed by titration with adsorbed oxygen and that chemisorbed by Pt after the oxygen is desorbed. Interpretation of the TPR data is not straightforward; some of the complexities have been summarized by Huizinga et al. (11).

The results of this experiment are consistent with the inference that Pt existed as Pt(IV) in the calcined Pt sample. Pt was completely reduced to the metallic state in the first temperature-programmed reduction. The results are consistent with the inference that during passivation, oxygen

chemisorption occurred on the reduced sample at room temperature. These results are consistent with those reported by Huizinga et al. (11).

Reduction behavior of γ-Al$_2$O$_3$-supported Re samples prepared from salt precursors and from organometallics. The sample of Re on γ-Al$_2$O$_3$ derived from NH$_4$ReO$_4$ was first dried at 500°C in He for 1 h to partially remove surface hydroxyl groups before the first reduction profile was obtained. A comparison could then be made with the sample prepared from [H$_3$Re$_3$(CO)$_{12}$] adsorbed on γ-Al$_2$O$_3$ that had been predried at 500°C.

The temperature corresponding to the maximum rate of reduction of the γ-Al$_2$O$_3$-supported calcined sample formed from NH$_4$ReO$_4$ was 438°C, but the H$_2$ consumption persisted even at 500°C, indicating that the reduction was incomplete (Fig. 4B). From the H$_2$ consumption, it is concluded that 69% of the Re was reduced to Re(0), whereby it has been assumed that all the Re existed as Re(VII) before reduction (Table 4). Moreover, the broadness of the reduction profile suggests that a spectrum of surface species might have existed.

The reduction profile of the passivated sample formed from the salt precursor exhibited a maximum at 390°C with a full width at half of the maximum height (FWHM) of 110°C (Fig. 4C). The H$_2$ consumption was determined to be 135 μmol of H$_2$/g of catalyst (Table 4), which is in close agreement with the amount of H$_2$ consumed in the calcined sample (129 μmol of H$_2$/g of catalyst). This result suggests that passivation had led to a complete oxidation of Re(0) to Re(VII) instead of a partial oxidation to Re(II). The complete oxidation of Re can be accounted for by the high affinity of Re for O; the oxophilic Re is known for its capacity for oxygen storage (48).

Although Re was present as high-valent oxides both after calcination and after passivation, the temperatures corresponding to the maximum rate of reduction were different for the two samples. The downshift of the reduction peak after passivation can be

TABLE 4

H₂ Consumption in TPR of Alumina-Supported Re–Pt Catalysts

Sample	H₂ Consumption (μmol of H₂/g of catalyst)	Calculated H₂ consumption[a] (μmol of H₂/g of catalyst)			
		Re^{2+}	Re^{4+}	Re^{6+}	Re^{7+}
Re on γ-Al₂O₃ derived from salt precursor[b]	129	54	108	161	188
Re on γ-Al₂O₃ derived from salt precursor (passivated)[b]	135	54	108	161	188
Re on γ-Al₂O₃ derived from [H₃Re₃(CO)₁₂] (passivated)	206	64	129	193	225
		Pt^{2+}		Pt^{4+}	
Pt on γ-Al₂O₃ derived from salt precursor	82	41		82	
Pt on γ-Al₂O₃ derived from salt precursor (passivated)	45	41		82	

[a] The calculated H₂ consumption is an estimated value of what would be needed to reduce the stated cationic species to the zerovalent state.
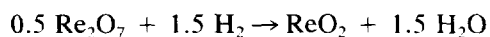
[b] Sample was dried at 500°C in He for 1 h prior to TPR.

explained by a weak interaction of the Re oxide with the alumina surface in the passivated sample. A TPR experiment with unsupported Re_2O_7 (heating rate = 10°C/min) gave a reduction peak at only 292°C (49). Thus the reduction behavior of Re in the calcined and in the passivated sample implies that Re cations strongly interact with alumina in the calcined sample and lead to a higher reduction temperature.
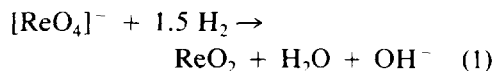
The reduction behavior of the passivated sample prepared from [H₃Re₃(CO)₁₂] adsorbed on γ-Al₂O₃ was similar to that of the supported Re sample prepared from the salt precursor. The reduction began at 193°C and reached a maximum in rate at 335°C (Fig. 4D). The total H₂ consumption was equivalent to a reduction of Re(VI) to Re(0) or a 92% reduction from Re (VII) to Re(0) (Table 4). The peak temperature was 55°C lower than that characteristic of the sample prepared from the salt precursor, but a second reduction peak appeared at 375°C. The peak heights are in the ratio 3 : 2 (low-temperature peak : high-temperature peak).

The origin of the reduction peaks might be

suggested to be associated with the stepwise reduction of Re(VII) to Re(IV) to Re(0). However, the relative ratio of the H₂ consumption based on the stoichiometry of Eq. (1) and Eq. (2) is expected to be 1.5 : 2 and does not agree with the reduction data:

$$0.5 \ Re_2O_7 + 1.5 \ H_2 \rightarrow ReO_2 + 1.5 \ H_2O$$

or

$$[ReO_4]^- + 1.5 \ H_2 \rightarrow$$
$$ReO_2 + H_2O + OH^- \quad (1)$$
$$ReO_2 + 2 \ H_2 \rightarrow Re + 2 \ H_2O. \quad (2)$$

This result implies that the two reduction peaks may be produced by two (or more) types of Re–O interactions in the sample after passivation. There is not enough information to allow an identification of the possible origins of the interactions. Similar types of Re–O interactions may exist in the γ-Al₂O₃-supported Re sample prepared from the salt precursor, but the heterogeneity of the surface species formed from the salt precursor resulted in a broad reduction peak.

In summary, complete oxidation of all the Re to Re(VII) took place during passivation as indicated by the H_2 consumption in the second reduction of the passivated samples. The passivated sample of Re on γ-Al_2O_3, prepared either from the salt precursor or the carbonyl cluster, was reduced at approximately 360°C in the absence of Pt. Since Re is easily oxidized by exposure to O_2 at room temperature, its oxophilic character may pose a problem when O_2 is used as an adsorbate to determine the exposed Re surface area in supported Re and Re–Pt catalysts.

The reduction profiles of calcined τ-Al_2O_3-supported Re–Pt samples prepared from salt precursors under two distinct sets of drying conditions were investigated. After the first temperature-programmed reduction experiment, the two samples were passivated at room temperature followed by a second reduction experiment to examine the influence of surface hydroxylation on their reduction behavior. The reducibility of a passivated Re–Pt sample formed from $[Re_2Pt(CO)_{12}]$ was also investigated to provide indirect structural information and compared with that of the two passivated Re–Pt samples prepared from the salt precursors.

The influence of the degree of hydroxylation on the reduction behavior of the calcined γ-Al_2O_3-supported Re–Pt sample prepared from the salt precursors was investigated. Prior to reduction, a sample was dried at 500°C in He for 1 h. Its reduction profile exhibited a broad peak with two maxima, at 308 and 405°C (Fig. 5A). The amount of H_2 consumed is only 46% of that required to reduce all the Pt from Pt(IV) to Pt(0) and the Re from Re(VII) to Re(0) (Table 5). In contrast, when the sample was dried at 120°C before reduction, a sharp reduction peak with a maximum at 263°C was observed (Fig. 5C). The FWHM was 60°C, but the peak tailed at high temperature. The H_2 consumption indicates that both the Re and Pt were reduced fully.

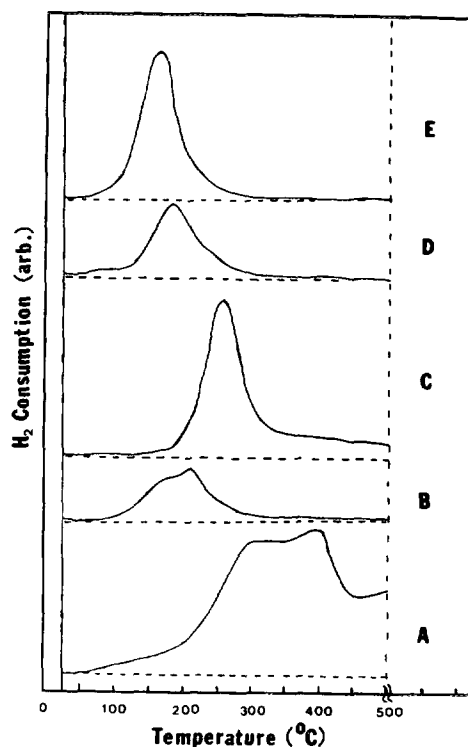There are reports of the dependence of the reduction behavior of the alumina-

FIG. 5. TPR profiles for (A) calcined γ-Al_2O_3-supported Re–Pt sample prepared from the salt precursors after He treatment at 500°C, (B) passivated form of this sample, (C) calcined γ-Al_2O_3-supported sample formed from salt precursors after He treatment at 120°C, (D) passivated form of sample C, and (E) passivated γ-Al_2O_3-supported sample formed from $[Re_2Pt(CO)_{12}]$.

supported samples on the drying temperature. The degree of surface hydroxylation has been proposed to affect the mobility of surface perrhenates, which migrate toward Pt (39). Alternatively, it may influence the rate of the hydrogen transfer from Pt to oxidized Re species via surface hydroxyl groups (41), resulting in the observed facilitated reduction of Re.

A downshift in the temperature for the maximum rate of reduction with respect to that obtained from the first reduction experiment was observed for the two passivated Re–Pt samples prepared from salt precursors. The sample that had been dried at 500°C exhibited a maximum reduction rate

TABLE 5

H₂ Consumption in TPR of Alumina-Supported Re–Pt Samples

| | | H₂ Consumption (μmol of H₂/g of catalyst) | | | | | | | |
| | | Calculated value[a] | | | | | | | |
Sample	Experimental result	$Pt^{2+}-Re^{2+}$	$Pt^{2+}-Re^{4+}$	$Pt^{4+}-Re^{4+}$	$Pt^{2+}-Re^{6+}$	$Pt^{2+}-Re^{7+}$	$Pt^{4+}-Re^{6+}$	$Pt^{4+}-Re^{7+}$
Re–Pt on γ-Al₂O₃ derived from salt precursors[b]	233	82	136	164	190	216	218	245
Re–Pt on γ-Al₂O₃ derived from salt precursors (passivated)	157	82	136	164	190	216	218	245
Re–Pt on γ-Al₂O₃ derived from salt precursors[c]	113	82	136	164	190	216	218	245
Re–Pt on γ-Al₂O₃ derived from salt precursors[c] (passivated)	93	82	136	164	190	216	218	245
Re–Pt on γ-Al₂O₃ derived from [Re₂Pt(CO)₁₂][b] (passivated)	212	82	137	164	192	219	219	246

[a] The calculated H₂ consumption is an estimate of what would be needed to reduce the stated pair of cationic species to the zerovalent state.
[b] The sample was dried at 120°C in He for 1 h prior to TPR.
[c] The sample was dried at 500°C for 1 h prior to TPR.

at 213°C with a FWHM of 95°C (Fig. 5B). In contrast, the sample that had been dried at 120°C exhibited a maximum reduction rate at 185°C with a FWHM of 75°C (Fig. 5D).

A tentative interpretation of the data can be made on the basis of the assumption that during the passivation Re is oxidized to Re(VII) and Pt is oxidized to Pt(II); these are the results observed with the monometallic samples.

The H₂ consumption of the sample that had been dried at 500°C is consistent with the inference that the Pt was oxidized to Pt(II) during the passivation and the Re that had not been reduced in the first reduction was still not reduced, but that the Re that had been reduced after the first reduction (and was reoxidized in the passivation) was (re-)reduced in the second reduction. The H₂ consumption of the sample dried at 120°C was less than that expected on the basis of assumptions stated in the preceding paragraph.

The reduction profile of the passivated γ-Al₂O₃-supported Re–Pt sample prepared from [Re₂Pt(CO)₁₂] adsorbed on γ-Al₂O₃ was different from those of passivated monometallic Re samples. The maximum rate of reduction occurred at 165°C with a FWHM of 60°C (Fig. 5E). Reduction commenced at 65°C and was completed at 330°C. H₂ consumption was observed at room temperature, indicating the titration of adsorbed oxygen with hydrogen on Pt. From the H₂ consumption data, it follows that Re was oxidized at least to Re(VI) and the Pt oxidation state was +2 after passivation (Table 5).

In summary, the TPR results lead to the following conclusions: The results of the first reduction experiments show that the drying temperature influenced the ease of reduction of Re in the salt-derived Re–Pt catalysts. This observation agrees with literature reports (37, 49, 50). After passivation, the catalyst dried at the low temperature was easily reduced at a low temperature, but the amount of H₂ consumption was less than that expected on the basis of the assumptions that (1) Re was totally oxidized to Re(VII), and (2) Pt was oxidized to Pt(II). Similarly, the catalyst dried at the high temperature (after passivation) was also easily reduced at a low temperature. The H₂ consumption indicated that the Re that had not been reduced in the first reduction was still not reduced in the second reduction, but the Re that had been reduced in the first reduction (and was reoxidized in the passiv-

ation), was (re-)reduced in the second re-
duction. The passivated Re–Pt sample de-
rived from the metal carbonyl cluster was
most easily reduced of all the samples
tested. The reduction data (for the passiv-
ated sample) are consistent with the full re-
duction [to Pt(0) and Re(0)] of a sample that
had been oxidized in the passivation step to
give Re(VI) and Pt(II).

Re–Pt alloy formation? Several pertinent
points presented in the literature regarding
the facilitated reduction of Re in the pres-
ence of Pt supported on Al_2O_3 are the fol-
lowing:

(1) Issacs and Petersen (39) interpreted
their data as an indication that the mobility
of Re (formed from perrhenate) on the Al_2O_3
surface depends on the degree of hydroxyla-
tion of the surface.

(2) Isaacs and Petersen (39) hypothesized
that Re–Pt alloy formation occurred at the
temperature corresponding to the maximum
rate of reduction indicated by the TPR.

(3) Mieville (41) suggested that surface
hydroxylation influences the rate of hydro-
gen spillover and that the rate of reduction is
controlled by the rate of hydrogen spillover.

Since the oxides of Re and Pt present on
the surface of the salt-derived sample after
calcination are immiscible, it is inferred that
the two metals were segregated at this stage
of the preparation.

Wagstaff and Prins (37), on the basis of
TPR results, concluded that oxidative treat-
ments led to segregation of Re and Pt, but
under mild conditions (e.g., at ca. 100°C)
(passivation) the rate of segregation was
low. Their results and interpretation do not
rule out the possibility that the alloy struc-
ture could be disrupted, with the resulting
metal oxides segregated but in the near
neighborhood of each other on the support.

This literature provides the basis for the
following interpretation of the TPR results
of the present work:

If Re–Pt alloy particles had been formed
at all, they would be expected to have
formed in the first reduction step, because

the second reduction step is no more severe
than the first. It is also inferred, on the basis
of the assumption that the Wagstaff and
Prins (37) hypothesis is correct, that the inti-
macy of the two metals on the surface was
not altered in the passivation step since this
was carried out under the mild conditions
referred to by Prins and Wagstaff. Since the
samples, following passivation, were ex-
posed to the atmosphere to rehydroxylate
the surfaces to give the same degree of hy-
droxylation in each, it is suggested that any
differences between the samples should be
attributed to properties other than the de-
gree of surface hydroxylation.

Therefore, the relative ease of reduction
of the cluster-derived sample (the one most
easily reduced, i.e., having the lowest tem-
perature for the maximum rate of reduction)
is inferred to be an indication of the relative
intimacy of the two metals in that sample.
The metals were evidently most closely as-
sociated with each other in this sample. Fur-
thermore, the H_2 consumption of the second
reduction of the Re–Pt cluster-derived sam-
ple indicates that Re and Pt were present in
the form of highly dispersed clusters after
the first reduction and were converted to
oxide clusters of Re and Pt when the sample
was passivated (13, 37). Re and Pt oxides
are immiscible so that the two metals were
segregated and probably remained close to
each other.

The unexpectedly low H_2 consumption
characterizing the passivated Re–Pt sample
formed from salts and dried at low tempera-
ture can be accounted for by the hypothesis
of the formation of relatively large Re–Pt
alloy particles. According to the hypothesis
of Isaacs and Petersen (39), the low reduc-
tion temperature of the sample indicates the
formation of Re–Pt alloy particles after the
first reduction. If large alloy particles had
been formed after the first reduction, the
oxidation step (passivation) would not have
disrupted the particles because oxygen-in-
duced segregation would have occurred
(34), because of the high affinity of Re for
O, leading to the formation of a layer of Re

oxide encapsulating a metallic Pt core (a cherry model). In this case, the extent of oxidation of Pt would be limited. In the second reduction, H_2 could diffuse easily through this Re oxide coating and become activated by the metallic Pt core at low temperature. Re oxide would then be reduced at a low temperature because of the ease of H_2 activation by Pt. Thus the Re–Pt sample derived from salt precursors should have the closest proximity of the Re oxide to Pt and would be expected to give the lowest reduction temperature among all samples tested. However, this speculation is in contrast to the conclusion that the cluster-derived Re–Pt sample has the closest interaction between the two metals, as indicated by the temperature of the reduction peak.

An alternative hypothetical structural model to account for the low H_2 consumption in the salt-derived Re–Pt sample is the following: Re and Pt were segregated after the first reduction. The Pt dispersion was very low, with less Pt surface area than in a highly dispersed Pt sample. Thus, only a limited extent of oxidation would have taken place on the surface of Pt during passivation and little H_2 was needed to reduce the oxidized Pt to the zerovalent state. To distinguish between these two hypothetical models, more structural information is needed to determine whether direct Re–Pt interactions existed in the salt-derived sample.

In summary, the degree of surface hydroxylation has a significant influence on the reduction profile of supported Re–Pt catalysts prepared from salt precursors. The temperature corresponding to the maximum rate of reduction of the sample after high-temperature drying was observed to be higher than that characteristic of the sample dried at low temperature. By passivating the sample after high-temperature drying followed by exposure to air to rewet the surface, a low-temperature reduction peak similar to that characterizing the sample dried at low temperature was observed. However, the reduction profiles of the samples being examined cannot give much structural information. Since the Re–Pt interaction is only a prerequisite for the observed catalyzed reduction of Re, no conclusion can be drawn about whether the Re and Pt existed as a highly dispersed surface alloy.

X-ray absorption spectroscopy has been used to characterize the surface structure of the cluster-derived and salt-derived catalysts after drying. The results are to be presented separately (4).

REFERENCES

1. Sterba, M. J., and Haensel, V., *Ind. Eng. Chem. Prod. Res. Dev.* **15**, 2 (1976).
2. Kluksdahl, H. E., U.S. Patent 3,415,737 (1968).
3. Fung, A. S., Kelley, M. J., Gates, B. C., and Koningsberger, D. C., submitted for publication.
4. Fung, A. S., Kelley, M. J., Koningsberger, D. C., and Gates, B. C., submitted for publication.
5. Andrew, M. A., Kirtley, S. W., and Kaesz, H. D., *Inorg. Synth.* **17**, 66 (1977).
6. Herberhold, M., Suss, G., Ellerman, J., and Gabelein, H., *Chem. Ber.* **111**, 2931 (1978).
7. Clark, H. C., and Manzer, L. E., *J. Organomet. Chem.* **59**, 411 (1973).
8. Urbancic, M. A., Wilson, S. R., and Shapley, J. R., *Inorg. Chem.* **23**, 2954 (1984).
9. Schmidt, S. P., Trogler, W. C., and Basolo, F., *Inorg. Synth.* **23**, 41 (1983).
10. Yao, H. C., and Shelef, M., *J. Catal.* **44**, 392 (1976).
11. Huizinga, T., van Grondelle, J., and Prins, R., *Appl. Catal.* **10**, 199 (1984).
12. McKenna, W. P., Higgins, B. H., and Eyring, E. M., *J. Mol. Catal.* **31**, 199 (1985).
13. Gallezot, P., Coudurier, G., Primet, M., and Imelik, B., in "Molecular Sieves II" (J. R. Katzer, Ed.), ACS Symposium Series, Vol. 40, p. 144. American Chemical Society, Washington, DC, 1977.
14. Braterman, P. S., "Metal Carbonyl Spectra," p. 192. Academic Press, New York, 1975.
15. Urbancic, M. A., Ph.D. dissertation, University of Illinois, Urbana, 1984.
16. Flitcroft, N., Huggins, D. K., and Kaesz, H. D., *Inorg. Chem.* **3**, 1123 (1964).
17. Kirlin, P. S., DeThomas, F. A., Bailey, J. W., Gold, H. S., Dybowski, C., and Gates, B. C., *J. Phys. Chem.* **90**, 4882 (1986).
18. Papile, C. J., and Gates, B. C., *Langmuir* **8**, 74 (1992).

19. Chang, J.-R., Gron, L. U., Honji, A., Sanchez, K. M., and Gates, B. C., *J. Phys. Chem.* **95**, 9944 (1991).

20. Lamb, H. H., Gates, B. C., and Knözinger, H., *Angew. Chem., Int. Ed. Engl.* **27**, 1127 (1988).

21. Bastein, A. G. T. M., Toolenaar, F. J. C. M., and Ponec, V., *J. Catal.* **90**, 88 (1984).

22. Peri, J. B., *J. Catal.* **52**, 144 (1978).

23. Fung, A. S., Tooley, P. A., Kelley, M. J., Koningsberger, D. C., and Gates, B. C., *J. Phys. Chem.* **95**, 225 (1991).

24. Kelley, M. J., Fung, A. S., McDevitt, M. R., Tooley, P. A., and Gates, B. C., *in* "Microstructures and Properties of Catalysts," (M. M. J. Treacy, J. M. White, and J. M. Thomas, Eds.), Materials Research Soc. Proc., Vol. III. Materials Research Society, Pittsburgh, 1988.

25. Tysoe, W. T., Zaera, F., Somorjai, G. A., *Surf. Sci.* **200**, 1 (1988).

26. Nguyen, H. H., Salvati, L., and Hercules, D. M., to be published.

27. Kirlin, P. S., Strohmeier, B. A., and Gates, B. C., *J. Catal.* **98**, 308 (1986).

28. Alnot, M., Cassuto, A., Ducros, R., Ehrhardt, J., and Weber, B., *Surf. Sci.* **114**, L48 (1982).

29. Godbey, D. J., and Somorjai, G. A., *Surf. Sci.* **202**, 204 (1988).

30. Onuferko, J. H., Short, D. R., and Kelley, M., *J. Appl. Surf. Sci.* **19**, 227 (1984).

31. Huizinga, T., van't Blik, H. F. J., Vis, J. C., and Prins, R., *Surf. Sci.* **135**, 580 (1983).

32. Wertheim, G. K., DiCenzo, S. B., and Youngquist, S. E., *Phys. Rev. Lett.* **51** (25), 2310 (1983).

33. Adkins, S. R., and Davis, B. H., *in* "Catalyst Characterization Science: Surface and Solid State Chemistry" (M. L. Deviney and J. L. Gland, Eds.),

ACS Symposium Series, Vol. 288, p. 57. American Chemical Society, Washington, DC, 1985.

34. Unger, W., and Baunack, S., *Surf. Sci.* **184**, L361 (1987).

35. Biloen, P., Helle, J. N., Verbeek, H., Dautzenberg, F. M., and Sachtler, W. M. H., *J. Catal.* **63**, 112 (1980).

36. Jones, A., and McNichol, B., "Temperature-Programmed Reduction for Solid Materials Characterization." Dekker, New York, 1986.

37. Wagstaff, N., and Prins, R., *J. Catal.* **59**, 434 (1979).

38. McNicol, B. D., *J. Catal.* **46**, 438 (1977).

39. Isaacs, B. H., and Petersen, E. E., *J. Catal.* **77**, 43 (1982).

40. Bolivar, C., Charcosset, M., Frèty, R., Primet, M., and Tournayan, L., *J. Catal.* **37**, 437 (1984).

41. Mieville, R. L., *J. Catal.* **87**, 437 (1984).

42. Johnson, M. F. L., and LeRoy, V. M., *J. Catal.* **35**, 434 (1974).

43. Webb, A. N., *J. Catal.* **39**, 485 (1975).

44. Johnson, M. F. L., *J. Catal.* **39**, 487 (1975).

45. Short, D. R., Khalid, S. M., Katzer, J. R., and Kelley, M. J., *J. Catal.* **72**, 288 (1981).

46. Ziemecki, S. B., Jones, G. A., and Michel, J. B., *J. Catal.* **99**, 207 (1986).

47. Huang, Y. J., Xue, J., and Schwarz, J. A., *J. Catal.* **111**, 59 (1988).

48. Gandhi, H. S., and Shelef, M., U.S. Patent Application No. 607,660 (1975).

49. Arnoldy, P., van Oers, E. M. Bruinsma, O. S. L., de Beer, V. H. J., and Moulijn, J. A., *J. Catal.* **93**, 231 (1985).

50. Charcosset, H., Frèty, R., Leclercq, G., Mendès, E., Primet, M., and Tournayan, L., *J. Catal.* **56**, 468 (1979).